Ⅳ．研究成果の刊行物・別刷

INDEX

【雑誌】

Zeniya T, Watabe H, Hayashi T, Ose T, Myojin K, Taguchi A, Yamamoto A, Teramoto N, Kanagawa M, Yamamichi Y, Iida H	Three-dimensional quantitation of regional cerebral blood flow in mice using a high-resolution pinhole SPECT system and ^{123}I-iodoamphetamine.	*Nucl Med Biol*	157
Matsubara K, Watabe H, Kumakura Y, Hayashi T, Endres CJ, Minato K, Iida H	Sensitivity of kinetic macro parameters to changes in dopamine synthesis, storage, and metabolism: a simulation study for [^{18}F]FDOPA PET by a model with detailed dopamine pathway.	*Synapse*	165
Zeniya T, Hirano Y, Tominaga T, Hori Y, Watabe H, Sakimoto T, Sohlberg A, Minato K, Hatazawa J, Iida H	Conceptual design of high spatial-resolution SPECT system for human brain	*2011 IEEE Nuclear Science Symposium Conference Record*	177
Harada, Y., Yamamoto, T., Sakai, M., Saiki, T., Kawano, K., Maitani, Y., Yokoyama, M..	Effects of organic solvents on drug incorporation into polymeric carriers and morphological analyses of drug-incorporated polymeric micelles.,	*Int J Pharm*	180
Shiraishi, K., Endoh, R., Furuhata, H., Nishihara, M., Suzuki, R., Maruyama, K., Oda, Y., Jo, J., Tabata, Y., Yamamoto, J., Yokoyama, M..	A facile preparation method of a PFC-containing nano-sized emulsion for theranostics of solid tumors. International	*Int J Pharm*	190
Yokoyama, M..	Clinical applications of polymeric micelle carrier systems in chemotherapy and image diagnosis of solid tumors.	*J Exp Clin Med*	199
Egashira Y, Takahashi JC, Ohnishi H, Kawasaki Y, Higashigawa M, Iihara K, Miyamoto S.	Surgical treatment and perioperative management of moyamoya disease associated with glycogen storage disease Type 1a.	*J Neurosurg Pediatr*	207
Funaki T, Iihara K, Miyamoto S, Nagatsuka K, Hishikawa T, Ishibashi-Ueda H.	Histologic characterization of mobile and nonmobile carotid plaques detected with ultrasound imaging.	*J Vasc Surg*	211
Huang Q, Zeniya T, Hirano Y, Kudo H, Iida H, Gullberg GT.	Evaluation of a brain imaging system with combined parallel hole and pinhole collimation	*Proceedings of 11th International Meeting on Fully Three-Dimensional Image Reconstruction in Radiology and Nuclear Medicine*	218
E.A.Rashed, H.Kudo	Row-action image reconstruction algorithm using lp-norm distance to a reference image	*Conference Record of 2011 IEEE Nuclear Science Symposium and Medical Imaging Conference*	222
E.A.Rashed, Z.Wang, H.Kudo	Adaptive thresholding for robust iterative image reconstruction from limited views projection data	*Conference Record of 2011 IEEE Nuclear Science Symposium and Medical Imaging Conference*	227
E.A.Rashed, H.Toda, T.Sera, A.Tsuchiyama, T.Nakano, K.Uesugi, H.Kudo	Towards a high-resolution local tomography using statistical iterative reconstruction	*Conference Record of 2011 IEEE Nuclear Science Symposium and Medical Imaging Conference*	231

E.A.Rashed, H.Kudo	Iterative thresholding framework for row-action reconstruction from sparse projection data	*Conference Record of 2011 IEEE Nuclear Science Symposium and Medical Imaging Conference*	235
Autio J, Kawaguchi H, Saito S, Aoki I, Obata T, Masamoto K, Kanno I.	Spatial frequency-based analysis of mean red blood cell speed in single microvessels: investigation of microvascular perfusion in rat cerebral cortex.	*PLoS One*	238
Autio JA, Kershaw J, Shibata S, Obata T, Kanno I, Aoki I.	High b-value diffusion-weighted fMRI in a rat forepaw electrostimulation model at 7 T.	*Neuroimage*	246
Takuwa H, Autio J, Nakayama H, Matsuura T, Obata T, Okada E, Masamoto K, Kanno I.	Reproducibility and variance of a stimulation-induced hemodynamic response in barrel cortex of awake behaving mice.	*Brain Res*	255
工藤博幸，イサムラシド	圧縮センシングを用いた少数方向投影データからのＣＴ画像再構成	*映像情報メディカル*	264
工藤博幸	脳イメージングにおける機能画像と形態画像融合の在り方－ＭＲＩ情報を利用したＳＰＥＣＴ／ＰＥＴ画像再構成法－	*日本医用画像工学会ＪＡＭＩＴ e-ニューズレター*	271
髙橋和晃，工藤博幸	ブロック反復型画像再構成における緩和パラメータを用いないリミットサイクル回避法－リストモード再構成への拡張	*日本医用画像工学会第30回大会論文集*	274
大森広崇，野村勇人，工藤博幸	脳血流ＰＥＴ／ＳＰＥＣＴイメージングにおける画像再構成と病変検出の統合	*日本医用画像工学会第30回大会論文集*	282

Journal of Cerebral Blood Flow & Metabolism (2012) 32, 844–850

www.jcbfm.com

Preserved acetazolamide reactivity in lacunar patients with severe white-matter lesions: ^{15}O-labeled gas and H_2O positron emission tomography studies

Tomohisa Nezu[1,2], Chiaki Yokota[1], Toshiyuki Uehara[1], Miho Yamauchi[3], Kazuhito Fukushima[4], Kazunori Toyoda[1], Masayasu Matsumoto[2], Hidehiro Iida[3] and Kazuo Minematsu[1]

[1]*Department of Cerebrovascular Medicine, National Cerebral and Cardiovascular Center, Suita, Japan;* [2]*Department of Clinical Neuroscience and Therapeutics, Hiroshima University Graduate School of Biomedical Sciences, Hiroshima, Japan;* [3]*Department of Bio-Medical Imaging, National Cerebral and Cardiovascular Center Research Institute, Suita, Japan;* [4]*Department of Radiology, National Cerebral and Cardiovascular Center, Suita, Japan*

Limited evidence exists on the relationships between severity of white-matter lesions (WMLs) and cerebral hemodynamics in patients without major cerebral artery disease. To examine changes of cerebral blood flow (CBF), oxygen metabolism, and vascular reserve capacity associated with severity of WML in patients with lacunar stroke, we used a positron emission tomography (PET). Eighteen lacunar patients were divided into two groups according to the severity of WMLs, assessed by Fazekas classification; grades 0 to 1 as mild WML group and grades 2 to 3 as severe WML group. Rapid dual autoradiography was performed with ^{15}O-labeled gas-PET followed by ^{15}O-labeled water-PET with acetazolamide (ACZ) challenge. Compared with the mild WML group, the severe WML group showed lower CBF (20.6 ± 4.4 versus 29.9 ± 8.2 mL/100 g per minute, $P = 0.008$), higher oxygen extraction fraction (OEF) (55.2 ± 7.4 versus 46.7 ± 5.3%, $P = 0.013$), and lower cerebral metabolic rate of oxygen ($CMRO_2$) (1.95 ± 0.41 versus 2.44 ± 0.42 mL/100 g per minute, $P = 0.025$) in the centrum semiovale. There were no significant differences in the ACZ reactivity between the two groups (48.6 ± 22.6% versus 42.5 ± 17.2%, $P = 0.524$). Lacunar patients with severe WMLs exhibited reduced CBF and $CMRO_2$, and increased OEF in the centrum semiovale. The ACZ reactivity was preserved in both patients with severe and mild WMLs in each site of the brain.
Journal of Cerebral Blood Flow & Metabolism (2012) **32,** 844–850; doi:10.1038/jcbfm.2011.190; published online 18 January 2012

Keywords: acetazolamide challenge; centrum semiovale; cerebrovascular reactivity; ischemic stroke; leukoaraiosis

Introduction

White-matter lesions (WMLs), observed as white-mater hyperintensity in T2-weighted magnetic resonance imaging or fluid-attenuated inversion recovery (FLAIR) image, are commonly observed among elderly people (Hachinski *et al*, 1987). However, they are also associated with hypertension, diabetes, and other vascular risk factors (Murray *et al*, 2005; Pantoni and Garcia, 1997). Development of WMLs is known to be a cause of cognitive impairment, dementia, and disability (Prins *et al*, 2005). Recent studies showed that WMLs are not only a stroke risk factor (Streifler *et al*, 2002) but also a predictor of unfavorable stroke outcome (Koton *et al*, 2009). Despite accumulating evidence of the clinical significance of WMLs, the pathogenesis of WMLs has not been fully clarified.

Healthy elderly subjects with severe WMLs were reported to have reduced cerebral blood flow (CBF) and preservation of oxygen metabolism

Correspondence: Dr C Yokota, Department of Cerebrovascular Medicine, National Cerebral and Cardiovascular Center, 5-7-1 Fujishiro-dai, Suita, Osaka 565-8565, Japan.
E-mail: cyokota@hsp.ncvc.go.jp
This study was supported in part by Research Grants for Cardiovascular Diseases (22-4-1) from the Ministry of Health, Labor, and Welfare of Japan; a Grant for Translational Research from the Ministry of Health, Labor, and Welfare of Japan; a Grant for Nano Medicine from the Ministry of Health, Labor, and Welfare of Japan; and a Grant-in-aid for Scientific Research from the Japan Society for the Promotion of Science.
Received 4 September 2011; revised 16 November 2011; accepted 28 November 2011; published online 18 January 2012

(Meguro *et al*, 1990). Patients with dementia of the Binswanger type have marked decrease of both CBF and oxygen metabolism in the white matter; however, patients without dementia have a lesser decrease in CBF with preservation of almost-normal oxygen metabolism (Yao *et al*, 1992). These findings indicated that chronic hypoperfusion due to the progression of small artery disease is associated with the development of WMLs. In addition, hemodynamic disturbance induced by internal carotid artery occlusive disease was suggested to contribute to the development of extensive WMLs (Yamauchi *et al*, 1999).

Limited evidence exists on the relationships between severity of WMLs and hemodynamic disturbance in patients without major cerebral artery occlusive disease. Some studies showed that vascular reactivity was not related to severity of WMLs (Birns *et al*, 2009; Turc *et al*, 1994). Other studies reported that vascular reactivity in patients with severe WMLs is impaired (Bakker *et al*, 1999; Chabriat *et al*, 2000; Fu *et al*, 2006; Isaka *et al*, 1994; Kozera *et al*, 2010; Mochizuki *et al*, 1997). These inconsistencies may be due to differences in modalities for evaluation of vascular reserve capacity; i.e., transcranial Doppler ultrasound (Bakker *et al*, 1999; Birns *et al*, 2009; Fu *et al*, 2006; Kozera *et al*, 2010), perfusion MRI (Chabriat *et al*, 2000), xenon inhalation computed tomography (Isaka *et al*, 1994; Mochizuki *et al*, 1997), and single photon emission computed tomography (Turc *et al*, 1994). There are also differences in the vasodilatory stimulus used; i.e., CO_2 inhalation (Bakker *et al*, 1999), breath holding, hyperventilation tests (Birns *et al*, 2009; Kozera *et al*, 2010), and acetazolamide (ACZ) challenge test (Chabriat *et al*, 2000; Fu *et al*, 2006; Isaka *et al*, 1994; Mochizuki *et al*, 1997; Turc *et al*, 1994). Although single photon emission computed tomography study with ACZ challenge can detect stage II hemodynamic failure (Powers, 1991) by positron emission tomography (PET) in patients with major cerebral artery occlusive disease (Hirano *et al*, 1994), the relationship between ACZ reactivity and oxygen metabolism in patients with WMLs without major artery disease has not been elucidated. We hypothesized that either impairment of vascular reserve capacity or chronic hypoperfusion in the white matter contributes to the development of WMLs without major artery disease.

The aim of this study was to examine the changes of CBF, oxygen metabolism, and vascular reserve capacity associated with the severity of WMLs in patients with lacunar stroke.

Materials and methods

Patients

This study was a single-center hospital-based prospective study. The study protocol was governed by the guidelines of national government based on the Helsinki Declaration revised in 1983, and it was approved by the Institutional Research and Ethics Committee of our hospital. All patients gave written informed consent to participate in the study. Patients with lacunar stroke, at least 3 weeks after the onset, were enrolled between April 2009 and April 2010. All patients underwent PET studies with ^{15}O-labeled gas ($C^{15}O_2$, $^{15}O_2$, $C^{15}O$) inhalation and ^{15}O-water with ACZ challenge autoradiography as described previously (Kudomi *et al*, 2005, 2007), as well as MRI studies. Lacunar stroke was defined as a typical clinical syndrome associated with a small infarct, <15 mm in diameter on MRI, restricted to the territory of a perforating artery without adjacent major artery occlusive lesions. Patients with stenosis ($>50\%$ in diameter) or occlusion of the internal carotid artery or the trunk of the middle cerebral artery on magnetic resonance angiography or ultrasonography were excluded from the study. The median time interval between the onset of stroke and PET studies was 1,017 days (interquatile range 519 to 1,856).

Baseline clinical characteristics including age, sex, hypertension, diabetes mellitus, dyslipidemia, and current smoking were recorded. Information of risk factors and medical history was collected from a self-reported medical history or inferred from prescribed medication by the primary physicians. Criteria for hypertension, diabetes mellitus, and dyslipidemia were as previously defined (Yokota *et al*, 2009). Cognitive function was evaluated in all patients by the mini-mental state examination (Folstein *et al*, 1975) and clinical dementia rating (Hughes *et al*, 1982). Dementia was defined as clinical dementia rating ≥ 1, and patients with dementia met the criteria proposed by National Institute of Neurological and Communicative Disorders and Stroke and the Alzheimer's Disease and Related Disorders Association (NINCDS-ADRDA Alzheimer's Criteria) (Roman *et al*, 1993).

Magnetic Resonance Imaging

Magnetic resonance imaging was performed on a 1.5-T scanner (Magnetom Vision or Magnetom Sonata; Siemens Medical Systems, Erlangen, Germany). The imaging protocol consisted of a T1-weighted spin-echo, a T2-weighted spin-echo, and FLAIR image. Severity of WMLs was assessed using the FLAIR (repetition time 900 ms, echo time 119 ms, field-of-view 230×201 mm^2, matrix 256×210, 4 mm slice thickness, and 2 mm gap between slices).

Two investigators (CY and TN), who were unaware of all clinical data, graded the degree of severity of WMLs by visual inspection using the Fazekas classification of WMLs as follows: none (grade 0), punctate (grade 1), early confluent (grade 2), and confluent lesions (grade 3) (Fazekas *et al*, 1987). The patients with grades 0 to 1 were defined as the mild WMLs group and those with grades 2 to 3 were defined as the severe WMLs group. Additionally, WMLs volume was measured manually based on FLAIR imaging (20 slices) using Dr View/LINUX software (AJS, Ver R2.5, Tokyo, Japan).

Positron Emission Tomography Imaging

We used an ECAT47 PET scanner (Siemens Medical Systems), which provided an intrinsic spatial resolution of 4.5 mm full-width at half-maximum at the center of the field-of-view. Data were acquired in 2D mode, and corrected for scatter compensation. A catheter was placed in the brachial artery for continuous monitoring of the arterial blood radioactivity concentration and arterial input function using a scintillator block detector system (BeCON; Molecular Imaging Labo, Suita, Japan) (Kudomi *et al*, 2003).

Quantitative images of CBF and oxygen extraction fraction (OEF) were obtained from a series of PET scans with ^{15}O-labeled gas ($C^{15}O_2$, $^{15}O_2$, and $C^{15}O$) inhalation after a rapid dual autoradiography protocol as reported in a series of publications by Kudomi *et al* (2005, 2007). Briefly, after a 10-minute transmission scan for the attenuation correction and an ^{15}O-labeled carbon monoxide ($C^{15}O$) scan for the blood volume assessment, a single dynamic scan was performed for 8 minutes, during which 4,000 MBq of oxygen ($^{15}O_2$) and 5,000 MBq of ^{15}O-labeled carbon dioxide ($C^{15}O_2$) gases were inhaled each >1 minute, sequentially at an interval of 5 minutes. Time to complete the whole dual autoradiography protocol was ~40 minutes. Cerebral metabolic rate of oxygen ($CMRO_2$) was calculated by multiplying the arterial oxygen content to the product images of OEF times CBF.

Additionally, two sets of PET scans were performed, each followed with ^{15}O-labeled water injection to assess regional CBF images using ^{15}O-water autoradiography (Kanno *et al*, 1987). The first scan was initiated without any pharmacological or physiological stress (at rest) and the second scan was performed at 10 minutes after an intravenous injection of ACZ titrated to 17 mg/kg. Physiological and laboratory data such as blood pressure, heart rate, and blood gas analysis (Siemens RAPIDLab 1265; Siemens Medical Systems) were obtained during the PET study.

Data Analysis

The small circular regions of interest (ROIs) (10 mm in diameter) were placed in the frontal cortex, parietal cortex, occipital cortex, basal ganglia, and centrum semiovale based on automatic registration of MRI to PET by using PVElab (the PVEOut Consortium) (Quarantelli *et al*, 2004; Svarer *et al*, 2005). The program is followed by automatic segmentation (running with Statistical Parametric Mapping 5 (SPM5) Software (Institute of Neurology, University College of London, London, UK) and correction of PET counts for fractional volume as determined from the segmentation. The ROIs were manually placed on the FLAIR images and transferred to the CBF images for analysis (Figure 1). We defined the ACZ reactivity as the percentage increase in CBF after ACZ administration relative to baseline CBF. In each subject, the mean measures were obtained by averaging the values for both hemispheres.

Statistical Analysis

Statistical analysis was performed using JMP 7.0 software (SAS Institute, Cary, NC, USA). The statistical significance of intergroup differences was assessed by χ^2 tests, unpaired *t*-tests, and the Mann–Whitney *U*-test, as appropriate. Logarithmic transformation was performed on WMLs volumes, which was a skewed variable. The relationship between each parameter of PET and log-WML was examined by Pearson's correlation. A value of $P<0.05$ was considered statistically significant.

Results

Patients were divided into two groups of severe WMLs ($n=9$) and mild WMLs ($n=9$) on the basis of MRI findings. There were no significant differences in age, sex, and vascular risk factors between the two groups (Table 1). Three patients with dementia defined as clinical dementia rating ≥1 were enrolled in the severe WMLs group; however, the rating of mini-mental state examination was not significantly different between the two groups. There were no significant differences in baseline CBF values between the gas-PET and H_2O-PET results. Compared with patients in the mild WMLs group, the patients

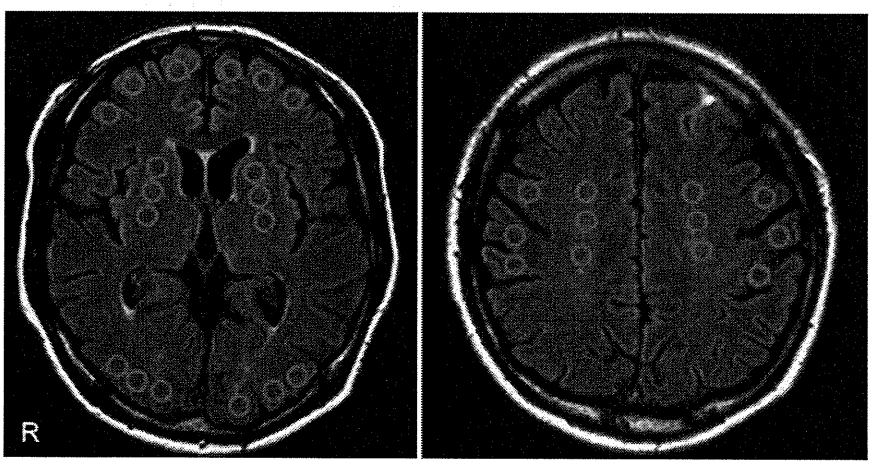

Figure 1 Regions of interest (ROIs) on fluid-attenuated inversion recovery (FLAIR). The small circular ROIs (10 mm in diameter) were placed on the frontal cortex, parietal cortex, occipital cortex, basal ganglia, and the centrum semiovale based on FLAIR image.

Table 1 Baseline characteristics

	Severe WMLs group (n = 9)	*Mild WMLs group (n = 9)*	P
Age (years)	76 (73–78)	74 (70–77)	0.329
Male	6 (67)	8 (89)	0.577
Current smoker	7 (78)	7 (78)	0.999
Hypertension	9 (100)	8 (88)	0.999
Diabetes mellitus	3 (33)	3 (33)	0.999
Dyslipidemia	6 (67)	6 (67)	0.999
WMLs (cm^3)	33.3 (21.5–90.9)	3.1 (1.3–4.4)	0.003
History of stroke	3 (33)	2 (22)	0.999
Time interval between stroke onset and PET study (days)	953 (445–1,958)	1,017 (519–1,623)	0.847
MMSE	24.0 (20.5–28.5)	28.0 (24.5–29.5)	0.140
CDR	0.5 (0–1)	0 (0–0.5)	0.185
Dementia	3 (33)	0 (0)	0.206

WMLs, white-matter lesions; PET, positron emission tomography; MMSE, mini-mental state examination; CDR, clinical dementia rating.
Data are number of patients (%), median (interquartile range) for discontinuous variables.

in the severe WMLs group had lower CBF (20.6 ± 4.4 versus 29.9 ± 8.2 mL/100 g per minute, $P = 0.008$), higher OEF (55.2 ± 7.4 versus 46.7 ± 5.3%, $P = 0.013$), and lower $CMRO_2$ (1.95 ± 0.41 versus 2.44 ± 0.42 mL/100 g per minute, $P = 0.025$) in the centrum semiovale, by gas-PET study (Table 2). There were no significant differences in any other parameters of the gas-PET in other ROIs between the two groups. Cerebral blood flow and $CMRO_2$ had a negative correlation with the severity of WMLs, and OEF had a positive correlation with the severity of WMLs (Figure 2). There were no significant differences in ACZ reactivity between the severe and mild WMLs groups in each site of the brain by H_2O-PET examination (Table 3). The results of physiological data and blood gas analysis during ACZ challenge were comparable between the two groups (data not shown). The ACZ reactivity was not correlated with the OEF or with the severity of WMLs ($P = 0.422$ and $P = 0.316$, respectively) (Figure 3).

Table 2 Comparison of each parameter of the gas-PET study between patients with severe or mild WMLs in the brain

	Severe WMLs group (n = 9)	*Mild WMLs group (n = 9)*	P
Frontal cortex			
CBF (mL/100 g per minute)	35.7 ± 9.0	37.8 ± 8.5	0.630
CBV (mL/100 g)	3.0 ± 0.9	3.0 ± 0.6	0.969
OEF (%)	54.1 ± 14.7	48.3 ± 5.2	0.275
$CMRO_2$ (mL/100 g per minute)	3.24 ± 0.49	3.26 ± 0.73	0.946
Parietal cortex			
CBF	40.2 ± 6.9	44.1 ± 11.6	0.403
CBV	2.8 ± 0.7	3.1 ± 0.5	0.284
OEF	50.6 ± 6.9	46.3 ± 4.9	0.146
$CMRO_2$	3.53 ± 0.35	3.62 ± 0.80	0.743
Occipital cortex			
CBF	40.4 ± 8.6	47.4 ± 16.1	0.266
CBV	3.5 ± 0.9	3.7 ± 1.5	0.745
OEF	55.8 ± 8.8	50.4 ± 4.5	0.116
$CMRO_2$	3.88 ± 0.63	4.22 ± 1.16	0.442
Basal ganglia			
CBF	45.1 ± 9.4	49.5 ± 13.1	0.426
CBV	2.3 ± 0.7	2.5 ± 0.5	0.521
OEF	52.8 ± 7.9	50.5 ± 6.3	0.505
$CMRO_2$	4.14 ± 0.66	4.43 ± 0.90	0.441
Centrum semiovale			
CBF	20.6 ± 4.4	29.9 ± 8.2	0.008
CBV	1.2 ± 0.4	1.4 ± 0.3	0.217
OEF	55.2 ± 7.4	46.7 ± 5.3	0.013
$CMRO_2$	1.95 ± 0.41	2.44 ± 0.42	0.025

CBF, cerebral blood flow; CBV, cerebral blood volume; $CMRO_2$, cerebral metabolic rate of oxygen; OEF, oxygen extraction fraction; PET, positron emission tomography; WMLs, white-matter lesions.
P value by Mann–Whitney *U*-test.

Discussion

This study showed reduced CBF, reduced $CMRO_2$, and increased OEF in patients with severe WMLs compared with those with mild WMLs in the centrum semiovale. All patients in this study had lacunar stroke without major cerebral artery disease. The study also showed that ACZ reactivity was not impaired in either the cortex or the white matter of the patients of both groups.

Hatazawa *et al* (1997) found asymptomatic WMLs subjects exhibited reduction of CBF in the white matter and basal ganglia without decrease in $CMRO_2$. They also observed an increase in OEF in these areas, suggesting a chronic hypoperfusion in these territories. The present study provided additional information of reduction of both CBF and $CMRO_2$ with an increase in OEF in the WML in the patient groups with severe WMLs. Centrum semiovale is located at the border of an area supplied by deep perforating arteries and the terminal branches of the middle cerebral artery. A decrease in CBF with reduction of $CMRO_2$ in the centrum semiovale in the present study should indicate a consequence of a reduced tissue metabolism in this terminal zone.

In the present study, patients with severe WMLs without major artery disease had increased OEF showed by gas-PET; however, their ACZ reactivity by H_2O-PET was preserved. The vascular reserve capacity evaluated by ACZ reactivity was preserved in both patients with severe and mild WMLs. Reduction of both CBF and $CMRO_2$ in the white matter was previously shown in patients with the Binswanger type dementia (Yao *et al*, 1990), being consistent with our results. Postmortem neuropathologic studies have shown decreased neuronal connectivity in the white matter in progressive subcortical vascular encephalopathy of Binswanger type (Yamanouchi *et al*, 1989, 1990). Functional reduction in cortical neuronal activity due to disruption of connections between the cortex and subcortex, as indicated previously (Pozzilli *et al*, 1987; Sette *et al*, 1989), is likely to be associated with a reduction of $CMRO_2$ in the centrum semiovale

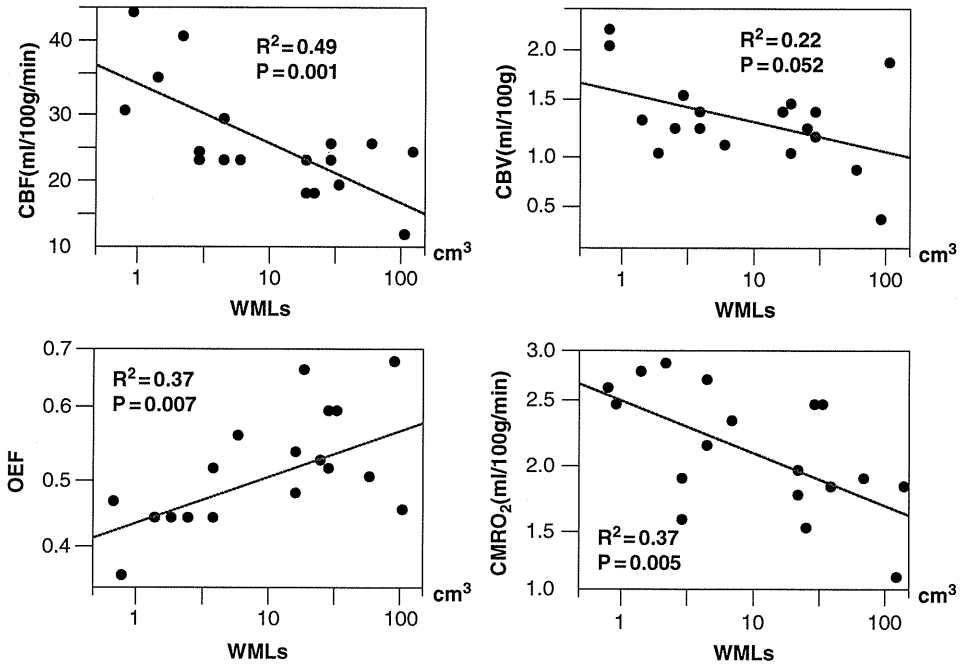

Figure 2 Correlation between WML volume and each gas-PET parameter in the centrum semiovale. CBF and $CMRO_2$ had a negative correlation with the severity of WMLs, while OEF was positively correlated with the severity of WMLs. CBF, cerebral blood flow; CBV, cerebral blood volume; OEF, oxygen extraction fraction; $CMRO_2$, cerebral metabolic rate of oxygen; WMLs, white-matter lesions; PET, positron emission tomography.

Table 3 Comparison of CBF between patients with severe or mild WMLs in the brain by H_2O-PET

	Severe WMLs group (n = 9)	*Mild WMLs group (n = 9)*	P
Frontal cortex			
CBF baseline	36.1 ± 7.2	40.2 ± 7.3	0.244
CBF ACZ	58.5 ± 10.2	59.9 ± 10.3	0.770
ACZ reactivity (%)	64.6 ± 28.5	49.7 ± 14.9	0.183
Parietal cortex			
CBF baseline	39.7 ± 4.8	45.7 ± 10.5	0.136
CBF ACZ	62.0 ± 7.1	66.9 ± 14.6	0.387
ACZ reactivity (%)	57.2 ± 17.1	47.1 ± 13.5	0.181
Occipital cortex			
CBF baseline	38.1 ± 7.1	45.7 ± 11.5	0.109
CBF ACZ	61.7 ± 13.3	70.1 ± 17.0	0.259
ACZ reactivity (%)	62.2 ± 21.5	54.2 ± 16.6	0.392
Basal ganglia			
CBF baseline	47.1 ± 9.8	54.6 ± 11.3	0.148
CBF ACZ	73.7 ± 10.5	85.7 ± 24.6	0.200
ACZ reactivity (%)	60.9 ± 31.0	55.7 ± 22.9	0.694
Centrum semiovale			
CBF baseline	19.0 ± 4.1	29.8 ± 9.2	0.005
CBF ACZ	28.5 ± 5.9	41.8 ± 10.9	0.005
ACZ reactivity (%)	48.6 ± 22.6	42.5 ± 17.2	0.524

ACZ, acetazolamide; CBF, cerebral blood flow; PET, positron emission tomography; WMLs, white-matter lesions.
P value by Mann–Whitney *U*-test.

in the patients with severe WMLs. Furthermore, the cerebral vessels would not dilate during fluctuations in systemic arterial pressure in daily life in these conditions of disruption of connections. Chronic hypoperfusion with a reduction of $CMRO_2$ in accordance with a disconnection between the cortex and subcortex may be the cause of development of WMLs without major artery disease.

To our knowledge, this is the first report of alterations in CBF, $CMRO_2$, and OEF, with preservation of ACZ reactivity in patients with mild or severe WMLs, with careful consideration of possible methodological errors. Indeed, quantitation of physiological parameters using PET is still a challenging issue, particularly in the white-matter area. As shown in earlier studies (Herscovitch and Raichle, 1983; Huang *et al*, 1987), the absolute values of both CBF and $CMRO_2$ could be biased because the spatial resolution of PET devices is limited compared with the physical size of the brain tissue component, or the partial volume effects. Oxygen extraction fraction is relatively stable and is less affected by partial volume effects. Our observation of increased OEF could not be explained by partial volume effects alone. Scatter is smaller in 2D mode in PET as compared with 3D acquisition. In this study, scatter correction was applied to minimize the contribution of radioactivity from the surrounding tissue components due to scatter. The ROIs were placed carefully with a guide of anatomical MRI to

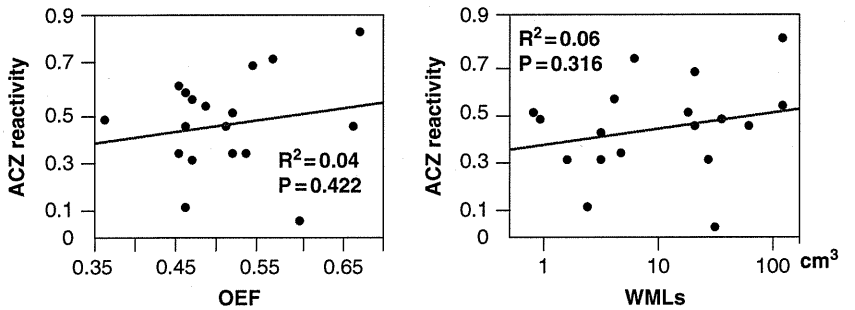

Figure 3 The correlation between ACZ reactivity and OEF or WML volume in the centrum semiovale. Neither OEF nor WML volume was correlated with ACZ reactivity. ACZ, acetazolamide; OEF, oxygen extraction fraction; WMLs, white-matter lesions.

minimize the errors arising from radioactivity counts of surrounding tissues. These factors remain concerns to be dealt with in future investigations.

There are several issues that need to be addressed, as follows. First, we intended to avoid possible bias in the patient selection, but a relatively small number of subjects could cause selection bias despite our efforts. Second, three patients with dementia were enrolled in the severe WMLs group. Because oxygen metabolism in demented patients was reported to be different from that in non-demented patients (Yao *et al*, 1992), a reduced $CMRO_2$ with reduced CBF in the severe WMLs group could be attributed to secondary effects arising from decreased cognitive function. Third, we examined the vascular reserve capacity by ACZ challenge. Recently, ACZ-induced vasodilation was reported not to inhibit the visually evoked flow response (Yonai *et al*, 2010), which indicates that the vasodilatory mechanism during neurovascular coupling may be different from the mechanism of ACZ-induced vasodilation. Acetazolamide at a dose of 17 mg/kg would not cause maximal cerebral vasodilatation. However, there were no significant differences in ACZ reactivity between the two groups, and ACZ reactivity was preserved in all patients in the present study. Fourth, PET imaging in the present study was a single scatter subtraction technique based on the Klein–Nishina formulation which was implemented in the reconstruction software (Watson, 2000). This technique was shown to provide reasonable accuracy in several phantom experiments. It should also be noted that the data were acquired in 2D mode, which has much smaller amount of scatter as compared with recently available 3D mode. Further, the filtered-back projection technique was applied for the image reconstruction. In this procedure, the scatter contribution is likely reduced in the reconstructed images. However, limited spatial resolution of PET devices is a significant source of errors that causes possible contamination of radioactivity counts of cortical grey matter tissue. Exact magnitude of errors in the calculated parameters in the WML cannot be well defined. In addition, PET scanning in the present study has not been applied to age-matched normal subjects. Further systematic study is needed.

In conclusion, we showed that there is reduced CBF and $CMRO_2$, and increased OEF in the centrum semiovale of patients with severe WMLs compared with patients with mild WMLs. The ACZ reactivity was preserved in both patients with severe and mild WMLs. Further studies will be needed to clarify the pathogenesis of WMLs.

Disclosure/conflict of interest

The authors declare no conflict of interest.

References

Bakker SL, de Leeuw FE, de Groot JC, Hofman A, Koudstaal PJ, Breteler MM (1999) Cerebral vasomotor reactivity and cerebral white matter lesions in the elderly. *Neurology* 52:578–83

Birns J, Jarosz J, Markus HS, Kalra L (2009) Cerebrovascular reactivity and dynamic autoregulation in ischaemic subcortical white matter disease. *J Neurol Neurosurg Psychiatry* 80:1093–8

Chabriat H, Pappata S, Ostergaard L, Clark CA, Pachot-Clouard M, Vahedi K, Jobert A, Le Bihan D, Bousser MG (2000) Cerebral hemodynamics in CADASIL before and after acetazolamide challenge assessed with MRI bolus tracking. *Stroke* 31:1904–12

Fazekas F, Chawluk JB, Alavi A, Hurtig HI, Zimmerman RA (1987) MR signal abnormalities at 1.5 T in Alzheimer's dementia and normal aging. *AJR Am J Roentgenol* 149:351–6

Folstein MF, Folstein SE, McHugh PR (1975) 'Mini-mental state'. A practical method for grading the cognitive state of patients for the clinician. *J Psychiatr Res* 12:189–98

Fu JH, Lu CZ, Hong Z, Dong Q, Ding D, Wong KS (2006) Relationship between cerebral vasomotor reactivity and white matter lesions in elderly subjects without large artery occlusive disease. *J Neuroimaging* 16:120–5

Hachinski VC, Potter P, Merskey H (1987) Leuko-araiosis. *Arch Neurol* 44:21–3

Hatazawa J, Shimosegawa E, Satoh T, Toyoshima H, Okudera T (1997) Subcortical hypoperfusion associated with asymptomatic white matter lesions on magnetic resonance imaging. *Stroke* 28:1944–7

Herscovitch P, Raichle ME (1983) Effect of tissue heterogeneity on the measurement of cerebral blood flow with the equilibrium C15O2 inhalation technique. *J Cereb Blood Flow Metab* 3:407–15

Hirano T, Minematsu K, Hasegawa Y, Tanaka Y, Hayashida K, Yamaguchi T (1994) Acetazolamide reactivity on ^{123}I-IMP single photon emission computed tomography in patients with major cerebral artery occlusive disease: correlation with positron emission tomography parameters. *J Cereb Blood Flow Metab* 14:763–70

Huang SC, Mahoney DK, Phelps ME (1987) Quantitation in positron emission tomography: 8. Effects of nonlinear parameter estimation on functional images. *J Comput Assist Tomogr* 11:314–25

Hughes CP, Berg L, Danziger WL, Coben LA, Martin RL (1982) A new clinical scale for the staging of dementia. *Br J Psychiatry* 140:566–72

Isaka Y, Okamoto M, Ashida K, Imaizumi M (1994) Decreased cerebrovascular dilatory capacity in subjects with asymptomatic periventricular hyperintensities. *Stroke* 25:375–81

Kanno I, Iida H, Miura S, Murakami M, Takahashi K, Sasaki H, Inugami A, Shishido F, Uemura K (1987) A system for cerebral blood flow measurement using an H215O autoradiographic method and positron emission tomography. *J Cereb Blood Flow Metab* 7:143–53

Koton S, Schwammenthal Y, Merzeliak O, Philips T, Tsabari R, Orion D, Dichtiar R, Tanne D (2009) Cerebral leukoaraiosis in patients with stroke or TIA: clinical correlates and 1-year outcome. *Eur J Neurol* 16:218–25

Kozera GM, Dubaniewicz M, Zdrojewski T, Madej-Dmochowska A, Mielczarek M, Wojczal J, Chwojnicki K, Swierblewska E, Schminke U, Wyrzykowski B, Nyka WM (2010) Cerebral vasomotor reactivity and extent of white matter lesions in middle-aged men with arterial hypertension: a pilot study. *Am J Hypertens* 23:1198–203

Kudomi N, Choi E, Yamamoto S, Watabe H, Kim K, Shidahara M, Ogawa M, Teramoto N, Sakamoto E, Iida H (2003) Development of a GSO detector assembly for a continuous blood sampling system. *IEEE Trans Nucl Sci* 50:70–3

Kudomi N, Hayashi T, Teramoto N, Watabe H, Kawachi N, Ohta Y, Kim KM, Iida H (2005) Rapid quantitative measurement of CMRO(2) and CBF by dual administration of (15)O-labeled oxygen and water during a single PET scan-a validation study and error analysis in anesthetized monkeys. *J Cereb Blood Flow Metab* 25:1209–24

Kudomi N, Watabe H, Hayashi T, Iida H (2007) Separation of input function for rapid measurement of quantitative CMRO2 and CBF in a single PET scan with a dual tracer administration method. *Phys Med Biol* 52:1893–908

Meguro K, Hatazawa J, Yamaguchi T, Itoh M, Matsuzawa T, Ono S, Miyazawa H, Hishinuma T, Yanai K, Sekita Y (1990) Cerebral circulation and oxygen metabolism associated with subclinical periventricular hyperintensity as shown by magnetic resonance imaging. *Ann Neurol* 28:378–83

Mochizuki Y, Oishi M, Takasu T (1997) Cerebral blood flow in single and multiple lacunar infarctions. *Stroke* 28:1458–60

Murray AD, Staff RT, Shenkin SD, Deary IJ, Starr JM, Whalley LJ (2005) Brain white matter hyperintensities: relative importance of vascular risk factors in nondemented elderly people. *Radiology* 237:251–7

Pantoni L, Garcia JH (1997) Pathogenesis of leukoaraiosis: a review. *Stroke* 28:652–9

Powers WJ (1991) Cerebral hemodynamics in ischemic cerebrovascular disease. *Ann Neurol* 29:231–40

Pozzilli C, Itoh M, Matsuzawa T, Fukuda H, Abe Y, Sato T, Takeda S, Ido T (1987) Positron emission tomography in minor ischemic stroke using oxygen-15 steady-state technique. *J Cereb Blood Flow Metab* 7:137–42

Prins ND, van Dijk EJ, den Heijer T, Vermeer SE, Jolles J, Koudstaal PJ, Hofman A, Breteler MM (2005) Cerebral small-vessel disease and decline in information processing speed, executive function and memory. *Brain* 128:2034–41

Quarantelli M, Berkouk K, Prinster A, Landeau B, Svarer C, Balkay L, Alfano B, Brunetti A, Baron JC, Salvatore M (2004) Integrated software for the analysis of brain PET/SPECT studies with partial-volume-effect correction. *J Nucl Med* 45:192–201

Roman GC, Tatemichi TK, Erkinjuntti T, Cummings JL, Masdeu JC, Garcia JH, Amaducci L, Orgogozo JM, Brun A, Hofman A, Moody DM, O'Brien MD, Yamaguchi T, Grafman J, Drayer BP, Bennett DA, Fisher M, Ogata J, Kokmen E, Bermejo F, Wolf PA, Gorelick PB, Bick KL, Pajeau AK, Bell MA, DeCarli C, Culebras A, Korczyn AD, Bogousslavsky J, Hartmann A, Scheinberg P (1993) Vascular dementia: diagnostic criteria for research studies. Report of the NINDS-AIREN International Workshop. *Neurology* 43:250–60

Sette G, Baron JC, Mazoyer B, Levasseur M, Pappata S, Crouzel C (1989) Local brain haemodynamics and oxygen metabolism in cerebrovascular disease. Positron emission tomography. *Brain* 112(Pt 4):931–51

Streifler JY, Eliasziw M, Benavente OR, Alamowitch S, Fox AJ, Hachinski VC, Barnett HJ (2002) Prognostic importance of leukoaraiosis in patients with symptomatic internal carotid artery stenosis. *Stroke* 33:1651–5

Svarer C, Madsen K, Hasselbalch SG, Pinborg LH, Haugbol S, Frokjaer VG, Holm S, Paulson OB, Knudsen GM (2005) MR-based automatic delineation of volumes of interest in human brain PET images using probability maps. *Neuroimage* 24:969–79

Turc JD, Chollet F, Berry I, Sabatini U, Démonet JF, Ceisis P, Marc-Vergnes JP, Rascol A (1994) Cerebral blood flow, cerebral blood reactivity to acetazolamide, and cerebral blood volume in patients with leukoaraiosis. *Cerebrovas Dis* 4:287–93

Watson CC (2000) New, faster, image-based scatter correction for 3D PET. *IEEE Trans Nucl Sci* 47:1587–94

Yamanouchi H, Sugiura S, Shimada H (1990) Loss of nerve fibres in the corpus callosum of progressive subcortical vascular encephalopathy. *J Neurol* 237:39–41

Yamanouchi H, Sugiura S, Tomonaga M (1989) Decrease in nerve fibres in cerebral white matter in progressive subcortical vascular encephalopathy of Binswanger type. An electron microscopic study. *J Neurol* 236:382–7

Yamauchi H, Fukuyama H, Nagahama Y, Shiozaki T, Nishizawa S, Konishi J, Shio H, Kimura J (1999) Brain arteriolosclerosis and hemodynamic disturbance may induce leukoaraiosis. *Neurology* 53:1833–8

Yao H, Sadoshima S, Ibayashi S, Kuwabara Y, Ichiya Y, Fujishima M (1992) Leukoaraiosis and dementia in hypertensive patients. *Stroke* 23:1673–7

Yao H, Sadoshima S, Kuwabara Y, Ichiya Y, Fujishima M (1990) Cerebral blood flow and oxygen metabolism in patients with vascular dementia of the Binswanger type. *Stroke* 21:1694–9

Yokota C, Minematsu K, Ito A, Toyoda K, Nagasawa H, Yamaguchi T (2009) Albuminuria, but not metabolic syndrome, is a significant predictor of stroke recurrence in ischemic stroke. *J Neurol Sci* 277:50–3

Yonai Y, Boms N, Molnar S, Rosengarten B, Bornstein NM, Csiba L, Olah L (2010) Acetazolamide-induced vasodilation does not inhibit the visually evoked flow response. *J Cereb Blood Flow Metab* 30:516–21

ORIGINAL ARTICLE

Effects of patient movement on measurements of myocardial blood flow and viability in resting ^{15}O-water PET studies

Kazuhiro Koshino, PhD,[a] Hiroshi Watabe, PhD,[b] Junichiro Enmi, PhD,[a] Yoshiyuki Hirano, PhD,[a] Tsutomu Zeniya, PhD,[a] Shinji Hasegawa, MD,[c] Takuya Hayashi, MD,[d] Shigeru Miyagawa, MD,[e] Yoshiki Sawa, MD,[e] Jun Hatazawa, MD,[b] and Hidehiro Iida, DSc[a]

Background. **Patient movement has been considered an important source of errors in cardiac PET. This study was aimed at evaluating the effects of such movement on myocardial blood flow (MBF) and perfusable tissue fraction (PTF) measurements in intravenous ^{15}O-water PET.**

Methods. **Nineteen ^{15}O-water scans were performed on ten healthy volunteers and three patients with severe cardiac dysfunction under resting conditions. Motions of subjects during scans were estimated by monitoring locations of markers on their chests using an optical motion-tracking device. Each sinogram of the dynamic emission frames was corrected for subject motion. Variation of regional MBF and PTF with and without the motion corrections was evaluated.**

Results. **In nine scans, motions during ^{15}O-water scan (inter-frame (IF) motion) and misalignments relative to the transmission scan (inter-scan (IS) motion) larger than the spatial resolution of the PET scanner (4.0 mm) were both detected by the optical motion-tracking device. After correction for IF motions, MBF values changed from 0.845 ± 0.366 to 0.780 ± 0.360 mL/minute/g ($P < .05$). In four scans with only IS motion detected, PTF values changed significantly from 0.465 ± 0.118 to 0.504 ± 0.087 g/mL ($P < .05$), but no significant change was found in MBF values.**

Conclusions. **This study demonstrates that IF motion during ^{15}O-water scan at rest can be source of error in MBF measurement. Furthermore, estimated MBF is less sensitive than PTF values to misalignment between transmission and ^{15}O-water emission scans. (J Nucl Cardiol 2012)**

Key Words: Myocardial blood flow • water-perfusable tissue fraction • PET • myocardial perfusion imaging • motion correction • ^{15}O-labeled water

INTRODUCTION

Positron emission tomography (PET) has been extensively utilized for a wide range of non-invasive functional imaging of the myocardium in vivo. When using this method, the global body movements of patients could be a source of quantitative errors. Such

From the Department of Investigative Radiology,[a] National Cerebral and Cardiovascular Center Research Institute, Osaka, Japan; Department of Molecular Imaging in Medicine,[b] Department of Cardiovascular Surgery,[e] Osaka University Graduate School of Medicine, Osaka, Japan; Department of Cardiology,[c] Osaka Kosei-nenkin Hospital, Osaka, Japan; Functional Probe Research Laboratory,[d] RIKEN Center for Molecular Imaging Science, Hyogo, Japan.

This study was supported by a Research Grant from the New Energy and Industrial Technology Development Organization (NEDO), Japan; a Grant for Translational Research from the Ministry of Health, Labour and Welfare (MHLW) of Japan; a Grant for Advanced Medical Technology from the Ministry of Health, Labour and Welfare (MHLW) of Japan; the Program for Promotion of Fundamental Studies in Health Science of the Organization for Pharmaceutical Safety and Research of Japan; and a Grant-in-Aid for Scientific Research from the Ministry of Education, Culture, Sports, Science and Technology (MEXT) of Japan.

Received for publication Apr 5, 2011; final revision accepted Jan 12, 2012.

Reprint requests: Kazuhiro Koshino, PhD, Department of Investigative Radiology, National Cerebral and Cardiovascular Center Research Institute, 5-7-1 Fujishirodai, Suita, Osaka 565-8565, Japan; *koshino@ri.ncvc.go.jp.*

1071-3581/$34.00

doi:10.1007/s12350-012-9522-0

Published online: 08 February 2012

movement could be particularly problematic when scans are carried out for a relatively long period.[1,2] Problems also arise when studies are carried out during physiologically stressed conditions, e.g., a cycling exercise in the PET scanner.[3] Errors can be attributed not only to the mismatch between the emission and the transmission data but also to the patient motion during each of the emission and/or the transmission scans.[3]

^{15}O-water PET studies provide quantitative information regarding myocardial blood flow (MBF) and coronary flow reserve (CFR), as well as a marker of myocardial viability, termed the water perfusable tissue fraction (PTF) or water perfusable tissue index (PTI).[4-12] The distribution of radioactivity during ^{15}O-water PET varies over time; this poses challenges for software-based correction of patient movement. Naum et al proposed to correct for such motion based on the rigid body model by aligning two external radioactive markers on the back of each subject. This study was conducted by performing dynamic scans while the subjects were under resting conditions and engaged in a cycling exercise.[3] Although no correction was made for the misalignment between transmission and emission scans, their study demonstrated reasonable improvement in calculated MBF values.

In our previous work, we developed an alternative system that uses an optical motion-tracking device to detect and correct for the patient's global movement during a cardiac ^{15}O-water PET study.[13] Our system provides a correction for movement during dynamic scanning, as well as for misalignment between the transmission and the emission scans, to compensate for errors in attenuation correction procedures. We evaluated and methodologically validated the inherent accuracy of this system in a cardiac phantom study. The correction for simulated global movement in a ^{15}O-water cardiac PET study of a healthy volunteer has also demonstrated reasonable regional MBF values, compared to values not adjusted for movement.

The purpose of this study was to evaluate the effects of global movements of subjects on quantification of MBF and PTF. Our previously validated system was used to detect and correct for the global movements of healthy volunteers, as well as patients who have suffered from severe cardiac dysfunction, during ^{15}O-water PET studies under resting conditions.

METHODS

Subjects

Subjects consisted of 10 healthy volunteers and 3 patients with previous myocardial infarction. The volunteers were all male, 22-32 years of age (mean ± 1standard deviation (SD) 25 ± 3 years). The volunteers had no signs or symptoms of ischemic heart disease. Patients were studied before and after the cell transplantation therapy with autologous myoblast sheets (AMS).[14,15] Scans were carried out by independent clinical research project, but were included in this study by mutual agreement. Two of the patients were male, the other was female; patients were 43-63 years of age. All patients had left ventricular assist systems (LVASs) at the time of PET study, except for one patient who received LVAS after the first PET and before the second PET studies. The PET studies were carried out 67-104 days (mean ± SD 82 ± 19 days) after the implantation of LVASs, and 26-106 days (mean ± SD 56 ± 44 days) after AMS transplantation therapy. All subjects gave written informed consent according to a protocol approved by the Ethical Committee and Internal Review Board of Osaka University.

PET Scan

The PET scanner was a HEADTOME-V tomograph (SHIMADZU Corp., Kyoto, Japan).[16] All data were acquired in 2D mode. Reconstructed images were obtained using a filtered back-projection algorithm with a Gaussian filter of 9 mm (full width at half maximum). The matrix and voxel sizes of reconstructed image were 128 × 128 × 63 and 2.03 × 2.03 × 3.13 mm^3, respectively. No scatter correction was applied to the image reconstruction.

Each subject was laid on the bed of the PET camera without any fixation of the body, and scanned at rest. A transmission scan was carried out first for correction of photon attenuation (20 minutes on the healthy volunteers, 10-15 minutes on the patients). A ^{15}O-CO emission scan for blood pool imaging was initiated 8 minutes after inhalation of ^{15}O-CO gas for 2 minutes (3.0-3.2 GBq). The ^{15}O-water dynamic emission scan was then carried out following intravenous administration of ^{15}O-water (1.1 GBq over 40 seconds) into the brachial vein, except for one patient who received the administration via right femoral vein. ^{15}O-water scans were performed for 6 minutes, using 26 dynamic frames consisting of 12 × 5 s, 8 × 15 s, and 6 × 30 s. ^{15}O-water scans were performed only once on eight healthy volunteers; two of the volunteers underwent ^{15}O-water scans twice. Thus, a total of twelve ^{15}O-water scans were carried out on the healthy volunteers. One patient underwent PET scans three times (before and after the implantation of LVAS, and after the cell transplantation therapy); the other two were scanned twice (before and after the cell transplantation therapy). Thus, a total of seven PET studies were carried out on the patients.

Motion Detection and Correction

Subject motion during cardiac ^{15}O-water PET was detected using an optical motion-tracking device, POLARIS (Northern Digital Inc., Canada). This method for motion correction (MC) is based on a rigid body model, and performed on each sinogram of the dynamic frame to correct for inter-scan (IS) and inter-frame (IF) motions, as shown in Figure 1. The correction process was performed automatically, based on

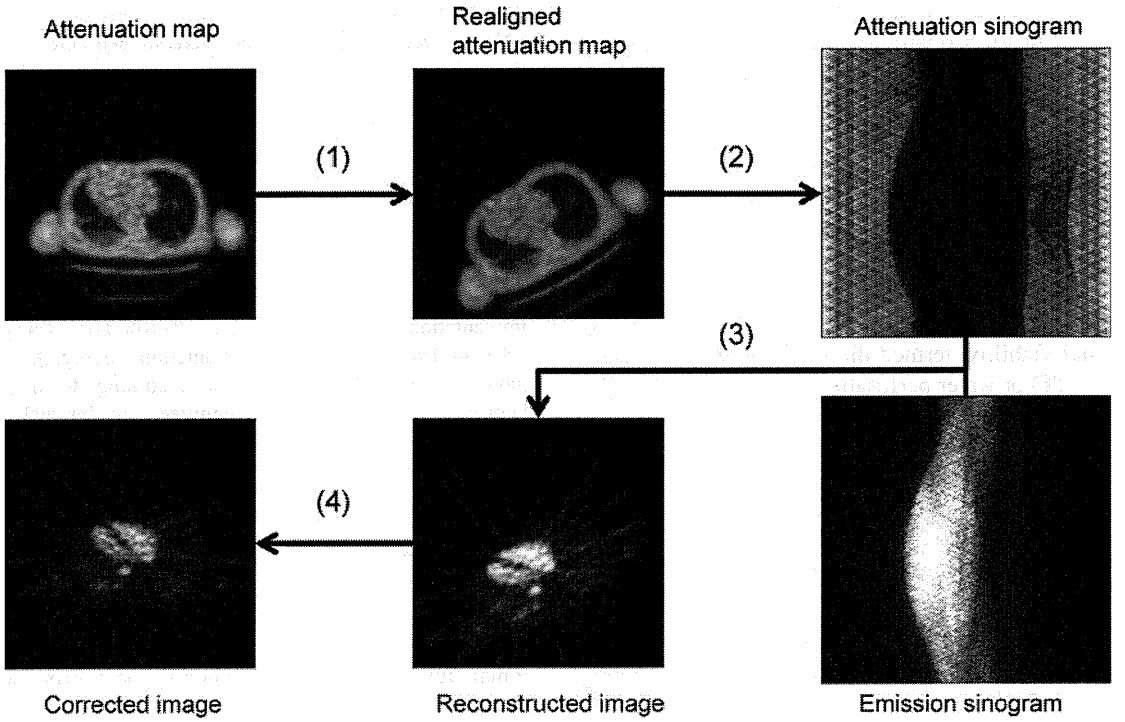

Figure 1. Schematic diagram of the correction for IS and IF motions.

user input consisting of subject locations measured by POLARIS, sinograms, and reconstruction parameters. In this manuscript, the IS motion denotes global motion between transmission and the first frame of ^{15}O-water emission scan; the IF motion, which is in addition to the IS motion, denotes global motion between frames of the ^{15}O-water scan. Methodological details regarding detection and correction of the motions are described in our previous studies.[13,17,18]

Motion Classification

Global movement during ^{15}O-water scan was characterized as consisting of IS and IF motions. Accordingly, motion was classified as: (1) IS + IF, in which both IS and IF motions were present; (2) IS motion only; (3) IF motion only; and (4) neither type of movement was present (NE). The presence of each IS and IF motion was determined as described below. Using values $t_x(i)$, $t_y(i)$, and $t_z(i)$ to represent translational movement in the x, y, and z, respectively, directions between the transmission and the ith frame of the ^{15}O-water scans, IS motion was considered significant if $\sqrt{t_x(1)^2 + t_y(1)^2 + t_z(1)^2} > 4.0\,\text{mm}$, where the value of 4.0 mm was the intrinsic spatial resolution of the PET scanner.[16]

IF motion was considered to be significant if $\max_i\{L(i), H(i)\} > 4.0\,\text{mm}$, where $L(i)$ represents the gradual movement of the subject during the scan, and $H(i)$ denotes the motion between adjacent frames. These two components of the IF motion can be expressed as

$$L(i) = \sqrt{\sum_{w=x,y,z} [t_w(i) - t_w(1)]^2} \tag{1a}$$

$$H(i) = \sqrt{\sum_{w=x,y,z} [t_w(i) - t_w(i-1)]^2} \tag{1b}$$

Motion Effect Evaluation

To evaluate motion effects on perfusion and viability measurements, we estimated regional MBF and PTF values for nine myocardial segments (anterior, lateral, posterior, and septal wall regions at middle and basal levels, as well as apex) with and without MCs, as described in the following section. Percent differences in the estimated values between with and without MCs for the nine myocardial regions were statistically tested using a one-way ANOVA to find myocardial segments sensitive to global movement. The percent differences were employed owing to avoiding difference of physiological states cross the subjects. The percent difference was defined by $\%\Delta q(i) = 100 \times |q_W(i) - q_{WO}(i)|/q_{WO}(i)$, where $q_W(i)$ and $q_{WO}(i)$ are MBF or PTF values, respectively, for the ith myocardial segment with and without MCs. Absolute values of MBF and PTF with and without MCs for each group were also assessed using Bland-Altman analysis and a paired 2-tailed t test. In the IS + IF motion group, to assess the effects of IS and IF motions, additional MBF and PTF estimations were performed on the data from ^{15}O-water images corrected for IS motions (IS + IF − IS) and also on data corrected for IF motions (IS + IF − IF). The quantitative values obtained from IS + IF − IS data were considered to be affected by IF

motion; likewise, values obtained from the IS + IF − IF data were considered to be affected by IS motion. The estimated values were compared to those without MCs using a paired 2-tailed t test. P values <.05 were considered statistically significant. Data was expressed as mean ± 1SD.

MBF and PTF Estimation

Regional MBF and PTF were obtained using the single tissue compartment model with correction for partial volume effects and spillover from the left ventricular cavity (LV)

$$C(t) = \text{MBF} \cdot \text{PTF} \cdot C_a(t) \otimes \exp\left(-\frac{\text{MBF}}{p}t\right) + V_a \cdot C_a(t)$$

where $C(t)$ represents the segment tissue time-activity curve (TTAC), $C_a(t)$ represents the arterial time-activity curve, p is the partition coefficient of water in the myocardial tissue (0.91 mL/g), and V_a is the arterial blood volume and spillover fraction from LV.[19] TTACs were generated for the nine myocardial segments using regions of interest (ROIs) selected within each ^{15}O-water myocardial image with and without MCs. The myocardial image was obtained by subtraction of the early phase of the dynamic ^{15}O-water image from the later phase. The midpoint between two phases was determined for each ^{15}O-water image using the contrast between myocardial regions and LV cavities. To obtain $C_a(t)$, a ROI was first drawn on a motion-corrected ^{15}O-CO image, without regard to whether MC had been applied to the ^{15}O-water image. The recovery coefficient of the LV was calculated from the ROI count on the ^{15}O-CO image and the blood radioactivity concentration. Second, the ROI was transformed to the ^{15}O-water image coordinate using a motion matrix that represents misalignment between transmission and the first dynamic frame of the ^{15}O-water scans. This transformation was made to evaluate motion effects on the ^{15}O-water scan, excluding effects of misalignment between ^{15}O-CO and ^{15}O-water scans. Using the transformed ROI, the LV TAC of the ^{15}O-water image was calculated. Finally, $C_a(t)$ was derived using the LV TAC and the overall TTAC was generated from nine myocardial segments according to the previous method.[6] To demonstrate the influence of IS motion, the ROI-based approach was not used; instead, pixel-by-pixel MBF and PTF values were estimated for a representative normal scan.[20] To denoise and smooth these parametric images, MBF and PTF were set to zero in voxels with PTF < 0.3 g/mL or V_a > 0.8 mL/mL, and then filtered using a Gaussian filter of 14 mm (full width at half maximum).[21] For normal scans in the group, improvement of homogeneity between myocardial segments by MC was also evaluated as $100 \times (1 - SD_W/SD_{WO})$, where SD_W and SD_{WO} were standard deviations of regional values with and without MCs, respectively.

RESULTS

Table 1 shows global movement during ^{15}O-water scans, categorized by the presence of IS and IF motions. Thirteen scans (7 scans on healthy volunteers and 6 scans on patients) exhibited IS motions greater than 4.0 mm, and 10 scans (5 scans on healthy volunteers and 5 scans on patients) exhibited IF motions greater than 4.0 mm. Among these, 4 scans on healthy volunteers and 5 scans on patients showed both IS and IF motions.

There was no statistically significant difference between the ROI volumes of ^{15}O-water images with and without MCs for IS, IF, and NE motion groups by paired 2-tailed t tests, and between the volumes with and without MCs, IS + IF − IS, and IS + IF − IF motion for IS + IF motion group by a one-way ANOVA.

Table 2 lists MBF and PTF values with and without MCs categorized by the four types of movement that occurred during ^{15}O-water studies, and average percent differences of MBF and PTF values over nine segments. Among 171 myocardial segments from all subjects, the fitting program failed to provide physiologically meaningful values in two segments (middle and basal septa for a healthy volunteer, in which IS + IF motion was detected) in the absence of MC. Those data were excluded from subsequent analysis. Among MBF values, significant changes by MCs were found in the IS + IF, IS + IF − IF, and IF motion groups: for IS + IF, from 0.845 ± 0.366 to 0.769 ± 0.319 mL/minute/g ($P < .05$); for IS + IF − IF, from 0.845 ± 0.366 to 0.780 ± 0.360 mL/minute/g ($P < .05$); and for IF, from 0.854 ± 0.179 to 1.088 ± 0.154 mL/minute/g ($P < .01$). PTF values in the IS motion group changed significantly from 0.465 ± 0.118 to 0.504 ± 0.087 g/mL ($P < .05$). This significant change is also shown in Figures 2 and 3, as differences between PTF values with and without MCs. In Figure 3, a data point indicated an averaged value for each scan.

Figure 4 illustrates the effect of IS motion of 5.0 mm on MBF and PTF of a normal subject from the IS motion group. The polar maps of normal PTF in Figure 4 demonstrate improvement of homogeneity in anterolateral regions by MC. Improvements of homogeneity of three normal scans in the group were 2.6% ± 26.1% for MBF and 30.9% ± 22.7% for PTF.

Table 1. Characteristics of motion during ^{15}O-water scans

Motion type	Total (normal) scans	IS motion (mm)	IF motion (mm)
IS + IF	9 (4)	7.7 ± 2.7	11.0 ± 4.0
IS	4 (3)	5.4 ± 1.0	2.8 ± 1.1
IF	1 (1)	2.7	5.1
NE	5 (4)	2.5 ± 0.7	1.4 ± 0.5

Table 2. The summary of MBF and PTF values with and without MCs

Motion type	Without MC	With MC	Percent difference
MBF (mL/minute/g)			
IS + IF	0.845 ± 0.366	0.769 ± 0.319*	33.8 ± 61.5
IS + IF − IS		0.815 ± 0.341	21.2 ± 38.5
IS + IF − IF		0.780 ± 0.360*	25.1 ± 41.4
IS	0.855 ± 0.343	0.828 ± 0.259	9.0 ± 8.9
IF	0.854 ± 0.179	1.088 ± 0.154†	30.2 ± 20.9
NE	0.898 ± 0.233	0.909 ± 0.221	9.7 ± 15.7
PTF (g/mL)			
IS + IF	0.476 ± 0.133	0.469 ± 0.128	13.9 ± 10.9
IS + IF − IS		0.471 ± 0.135	12.3 ± 13.0
IS + IF − IF		0.490 ± 0.119	12.3 ± 10.2
IS	0.465 ± 0.118	0.504 ± 0.087*	9.0 ± 9.6
IF	0.512 ± 0.067	0.483 ± 0.068	7.1 ± 5.6
NE	0.488 ± 0.095	0.496 ± 0.100	5.1 ± 4.9

IS, Inter-scan; *IF*, inter-frame.
NE denotes motion ≤4.0 mm. IS + IF − IS and IS + IF − IF represent IS + IF motion groups with correction of IS and IF motions, respectively.
* $P < .05$, † $P < .01$ vs without MC.

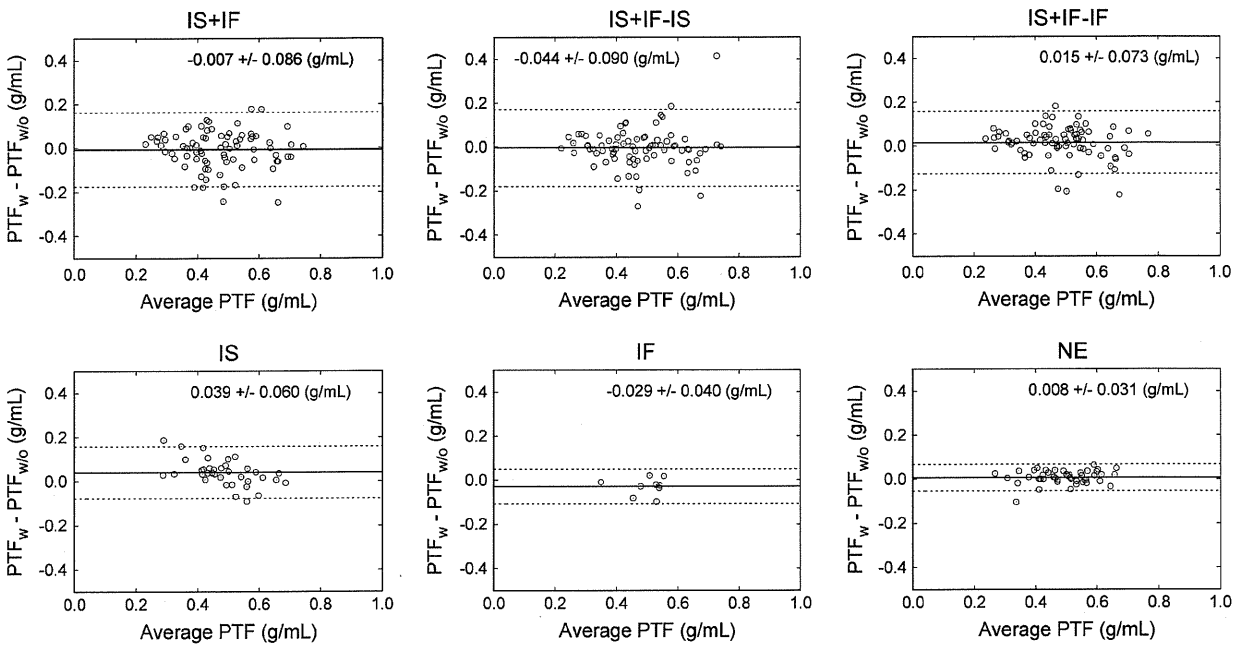

Figure 2. Differences between PTF values with and without the motion corrections. *IS*, Inter-scan motion; *IF*, inter-frame motion; *NE*, no significant motion. IS + IF − IS and IS + IF − IF are groups corrected for IS and IF motion in the IS + IF group, respectively.

Relative variability of regional MBF and PTF values due to global motion are shown in Figures 5 and 6, respectively. For MBF and PTF values in each motion group including the IS + IF − IS and IS + IF − IF groups, no significant difference between myocardial segments was observed in a one-way ANOVA (IF

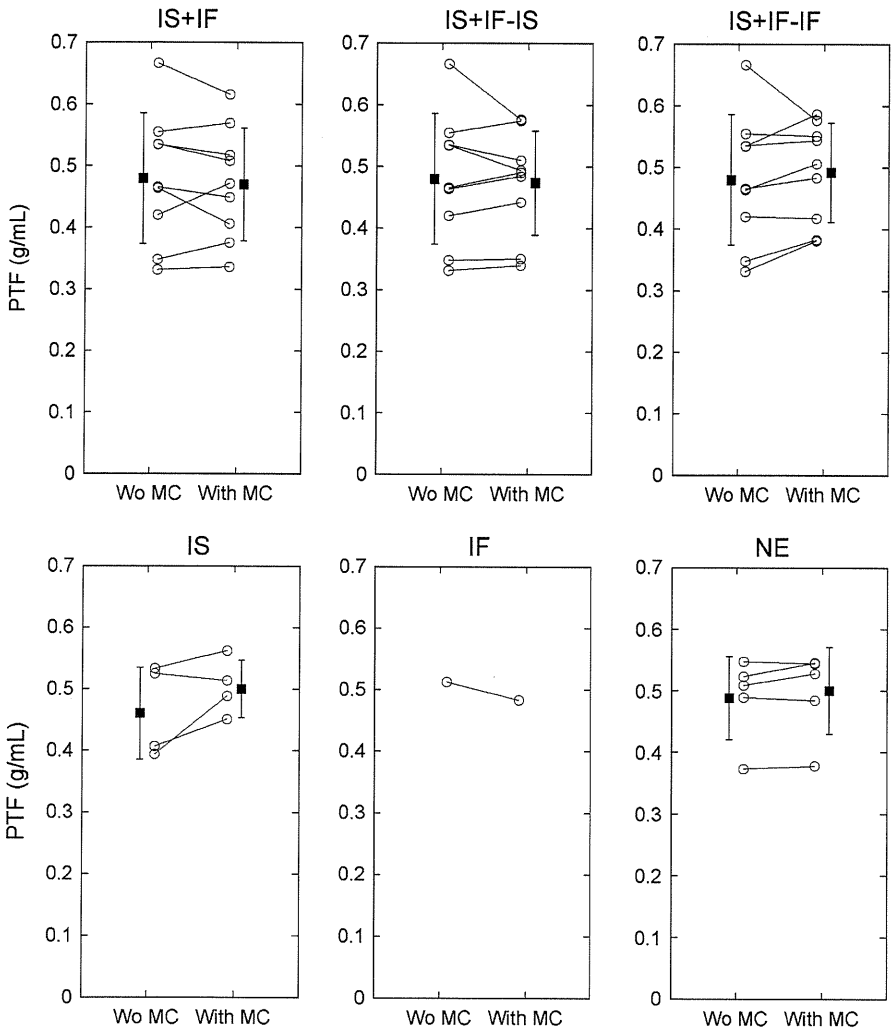

Figure 3. Changes in PTF values in the absolute scale by the MCs. *IS*, Inter-scan motion; *IF*, inter-frame motion; *NE*, no significant motion. IS + IF − IS and IS + IF − IF are groups corrected for IS and IF motion in the IS + IF group, respectively. A data point indicates an averaged value for each scan.

motion group was excluded from this analysis because one scan was assigned to this group. Data for IS + IF − IS and IS + IF − IF group were not shown).

DISCUSSION

In this study, global movements of the subjects during ^{15}O-water PET scans at rest were categorized as IS and IF motions. IS motion involves misalignment relative to the transmission scan, whereas IF motions involves changes between the dynamic frames during the ^{15}O-water scan. After categorization, the effects of these motions on MBF and PTF measurements were evaluated. Consequently, it was demonstrated that MBF values are affected by IF motion rather than IS motion.

Investigation of regional sensitivity to global movement resulted in no significant difference in regional MBF or PTF. This is because the direction and the magnitude of global movement varied for each subject; under- and over-estimation of MBF and PTF due to the motion could have occurred in any myocardial region. In this study, we utilized a one-way ANOVA to detect segmental differences. Due to small sample sizes, the ANOVA may fail to detect the differences. Correlation between segmental differences and the directions of global motions, especially IS motion, effects of which have been reported for misregistration between CT

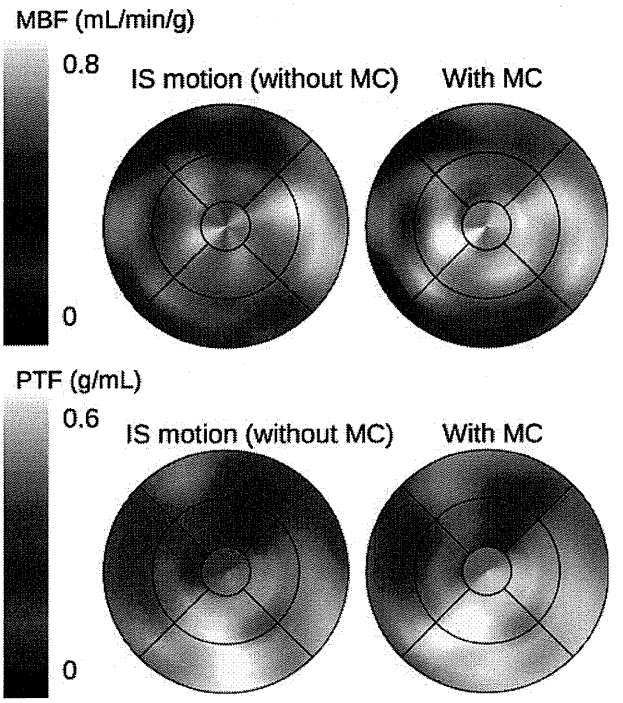

Figure 4. Effect of an IS motion of 5.0 mm on MBF and PTF of a normal subject in IS motion group.

attenuation map and emission image,[22,23] could be observed in large population study.

MBF values changed significantly upon correction for IF motions in the IF, IS + IF, and IS + IF − IF motion groups. In contrast, correction of IS motion was considered to have little effect, based on the results from the IS + IF − IS and IS motion groups in Table 2. It was further demonstrated that IF motion, but not IS motion, was an important source of error in the MBF measurement. The significant but small changes in MBF of IF, IS + IF, and IS + IF − IF motion groups after MCs could be due to the relatively large number of healthy volunteer scans in each group (1 of 1 scan for IF, 4 of 9 scans for IS + IF, respectively), as shown in Table 1. Suppression of IF motion during the ^{15}O-water scan is needed for accurate MBF measurement. For the IS motion groups, no significant change in MBF values and significant change in PTF values were observed by MCs (Figures 2, 3). For the normal scans in the group, the improvement of regional homogeneity was also observed in PTF rather than MBF. This is because the MBF values obtained using the kinetic model employed in this study were based on a clearance rate assessment of ^{15}O-water rather than the uptake rate of the radiotracer.[5] This is consistent with the findings of Lubberink et al,[21] who reported that MBF values do not change even if attenuation correction is omitted; this correction only caused changes in the absolute scale of TTAC, which then caused changes in PTF values. IS motions were also detected in the IS + IF motion group. For the IS + IF − IS motion group, in which IS motions were corrected, no significant change in PTF values was observed after MCs. This might be because IS and IF motions affected the ^{15}O-water images not subjected to MC in such a way as to cancel out errors in PTF measurements. PTF values were considered to be more affected than MBF values during the wash-in phase. However, in our study, IF motion had little effect on PTF values for the IS + IF − IF and IF groups, as shown in Table 2. The reasons for this discrepancy are follows: (1) to estimate the quantitative values, a nonlinear least squares method with same weights for all data points were applied to the data corrected for the physical decay. This fitting manner could be sensitive to radioactivity concentration in wash-out phase rather than wash-in phase. (2) Over-estimation in TTAC was introduced by contamination of the LV cavity count, using the ROI for TTAC superimposed on dynamic frames. However, the spillover correction could suppress the influence of IF motion. One of the advantages of ^{15}O-water over other cardiac PET tracers is that perfusion and viability measurements can be obtained from a single PET scan with short duration. Because accurate PTF measurement enabled assessment of

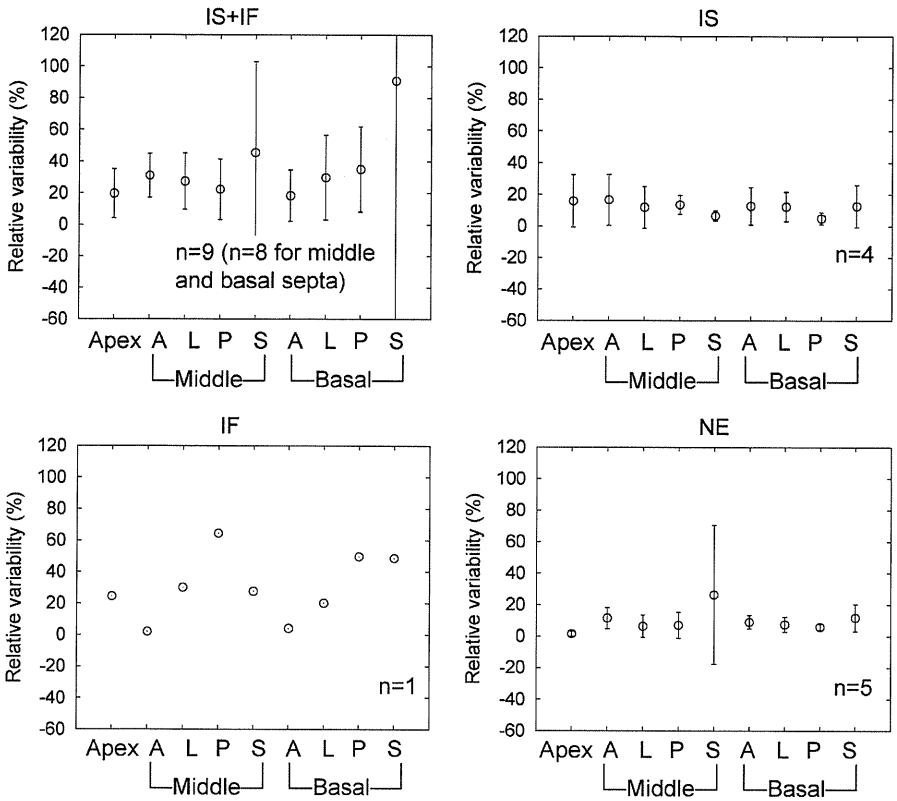

Figure 5. Relative variability of regional MBF due to effects of global motion. *IS*, Inter-scan motion; *IF*, inter-frame motion; NE represents no significant motion. IS + IF − IS and IS + IF − IF are groups corrected for IS and IF motion in the IS + IF group, respectively.

myocardial viability,[7-12] correction of IS motion, the effect of which was shown as the improvement of regional homogeneity of normal PTF in Figure 4, is considered to be important in the diagnosis of myocardial infarction, or evaluation of effects of cell transplantation therapies.

In this study, we performed ^{15}O-CO scans to determine a recovery coefficient for each subject.[5,6] ^{15}O-water PET studies without ^{15}O-CO scans have been reported in previous papers[3,21,24]; in these studies, the recovery coefficient could be fixed, or assumed to have a constant value. Omission of the ^{15}O-CO scan shortened the examination time, and might reduce motion artefacts. However, we considered that the adequacy of using a fixed recovery coefficient is still an unresolved issue in ^{15}O-water PET. We considered that the changes in MBF and PTF resulting from MCs were due to correction for global motion, and not due to variability of myocardial tissue ROIs drawn manually on ^{15}O-water images. We employed nine segmented regions rather than 17-segment AHA standard model for suppressing relatively large noise level of ^{15}O-water data.[4] In addition, the volumes of the ROIs for each motion group before and after MCs were almost equal (not statistically significant). Furthermore, lower sensitivity of MBF values to variation in ROI size and shape was demonstrated by Iida et al.[4] In this study, global motion might have occurred because subjects were scanned without any fixation. Although tight fixation prevents patient motion, such fixation could bring discomfort or pain to the patient; subsequent reaction to such pain could itself induce motion.

One limitation of this study is that all subjects were scanned at rest. When pharmacological or physiological stressors are administered, motion artefacts could be induced, as shown by Naum et al[3] in the context of physiological stress conditions. Our finding that MBF was sensitive to IF motion rather than IS motion was considered to be valid for a stress study; IF motion might be source of severe error in MBF and CFR measurements. The rigid body model, which was used in this study, has been promoted for motion compensation not only in brain PET but also in cardiac PET. McCord et al[1] employed the rigid body model to correct for misalignment during the transmission and ^{18}F-fluorodeoxyglucose (^{18}F-FDG) emission scans. Bacharach et al[2]

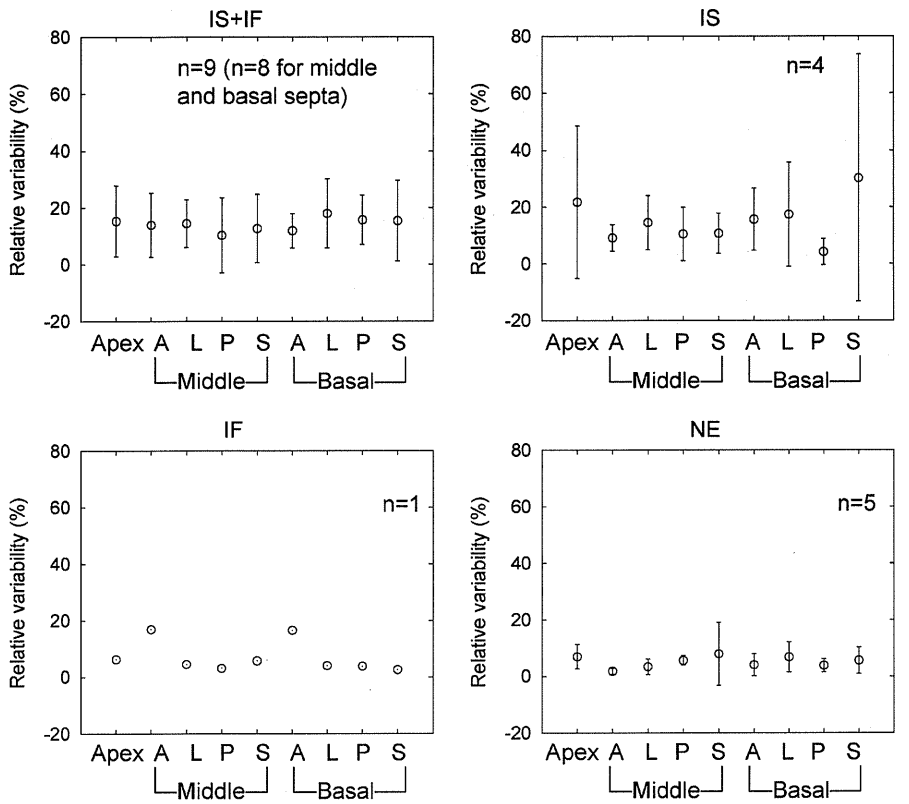

Figure 6. Relative variability of regional PTF due to effects of global motion. *IS*, Inter-scan motion; *IF*, inter-frame motion; NE represents no significant motion. IS + IF − IS and IS + IF − IF are groups corrected for IS and IF motion in the IS + IF group, respectively.

also proposed a registration technique based on the rigid body model for ^{18}F-FDG emission images acquired on different days. The use of the rigid body model is considered to be valid for non-gated cardiac PET images because the images were smoothed spatially due to cardiac wall motion, and also averaged temporally over the duration of the dynamic frames. However, in stress studies, over-correction due to relatively large respiratory motions might be introduced by our system because the subject's motion was estimated by measurement of the location of a target attached on the thoracic surface. With this in mind, further work is necessary to evaluate the contribution of MC in combination with a respiratory gating technique.

The MC system was applied to clinical follow-up studies of the patients who received LVAS and cell transplantation therapy. The aim of this study was to investigate the effects of global movement on quantification of MBF and PTF values in a single ^{15}O-water PET study under resting conditions. Although, we believed that the MC system could contribute to an accurate evaluation of regional perfusion and viability, the effects of LVAS implantation and AMS transplantation therapy on those patients is beyond the scope of the present study, and will be studied elsewhere.

CONCLUSIONS

This study demonstrated that IF motion during ^{15}O-water scans under resting conditions could be the source of error in MBF measurement. Furthermore, estimated MBF values were less sensitive than PTF values to misalignment between the transmission and the ^{15}O-water emission scans.

Acknowledgments

The authors are much indebted to the technical staff of the Department of Radiology, Osaka University Hospital, for their assistance. This study was supported by a Research Grant from the New Energy and Industrial Technology Development Organization (NEDO), Japan; a Grant for Translational Research from the Ministry of Health, Labour and Welfare (MHLW) of Japan; a Grant for Advanced Medical Technology from the Ministry of Health, Labour and Welfare (MHLW) of